Ilkogretim Online - Elementary Education Online, Year; Vol 20 (Issue 4): pp. 307-319
http://ilkogretim-online.org
doi: 10.17051/ilkonline.2021.04.33

Micropolar Squeeze Film Lubrication Analysis between Rough Porous Elliptical Plates and Surface Roughness Effects under the MHD

Brinda Halambi, Assistant Professor, Department of Mathematics, School of Applied Sciences, REVA University, Bangalore-560064, Karnataka, India, e-mail: brindahalambi@gmail.com
Hanumagowda B.N, Department of Mathematics, School of Applied Sciences, REVA University, Bangalore-560064, Karnataka, India**,** e-mail: hanumagowda.bn@reva.edu.in

Abstract- The present article theoretically analyses the impact of surface roughness and micropolar lubricant between two elliptical plates under the application of an external transverse magnetic field. An upper plate has a smooth surface, and a fixed lower plate has a porous material and roughness pattern. The film region of thickness H_1, composed of a nominal smooth and rough component, bridges the gap between the bearings and is filled with a non-Newtonian micropolar lubricant that is viscous, incompressible, and electrically conducting. For a one-dimensional longitudinal roughness pattern, the related stochastic Reynolds equation is obtained in the film region and solved analytically.Squeeze film characteristics, such as pressure distribution, load- carrying capacity, and squeeze film time of the bearings approach, are analyzed in the results. Squeeze film characteristics are increasing significantly for non-Newtonian micropolar and large roughness parameters and Hartmann numbers. These, on the other hand, are decreasing compared to the corresponding classical case for increasing permeability parameters. Nevertheless, as with the magnetic field, the higher values of the fluid gap number and coupling number also improve the lubrication properties.

Keywords: micropolar, Porous Elliptical Plates, magnetic field

I. INTRODUCTION

Magnetohydrodynamics (MHD) is a basic framework that analyses the dynamics of magnetic fields in electrically conducting fluids underlying the physical-mathematical system. MHD's key principle is that magnetic fields can induce currents in a moving conductive fluid, create fluid forces and alter the strengths of the geometry and magnetic fields. Due to the significant industrial significance of MHD, such as MHD pumps, MHD generators, etc., many researchers are inspired to work on MHD. We can find a variety of theoretical studies in literature on squeeze film bearings with the MHD effect. Kuzma [1] and Kuzma et al. [2] examined the behaviour of the squeeze film hydromagnetic theory, Shukla [3] researched the efficiency of the squeeze film magnetohydrodynamic theory for lubricant conduction, and several researchers [4-10] analyzed the performance of the hydromagnetic squeeze film between parallel plates of different bearings. All these studies have shown that the effect of the Hartmann number is to increase pressure, load-carrying capacity and squeezing time. In industry and engineering, theoretical and applied experimentation in micropolar fluid flow has attracted interest for a few decades; micropolar fluids generating micro rotational effects and micro rotational inertia are a subclass of micro fluids. To understand the flow behaviour of the micropolar fluid, the micro-continuum theory was developed by Eringen [11]. Experiments with various bearings and boundary conditions were studied by Aelen and Kline [12], Shukla and Isa [13], Roopa et al. [14], Naduvinamani and Huggi [15], Brinda and Hanumagowda [16], Siddanagouda and Patil [17], Prawal and Chandan [18], Isa and Zaheerudhin [19] and Roopa et al. [20]. Their studies show that improving the load carrying capacity and squeezing time is the result of micropolar lubricant.

In general, surface roughness and porosity play an important role in the characteristics of squeeze films. Shorter frequency of real surface relative to the troughs determines surface roughness. Each component's microscopic asperity greatly affects it. Differences in roughness are visibly different; however, they also influence the amount of wear, the ability to form a seal when a piece meets another surface, etc. A stochastic approach was developed by Christensen for the study of roughness in hydrodynamic lubrication [21]. A porous medium is characterized by the material carrying pores; they are typically full of fluid. In daily usage, much of the machinery has porous bearings to reinforce a revolving shaft. These bearings play an important role when dealing with noise, lubricant loss, premature failure, and intermittent friction. Surface resistance and porous media have made significant advances in the case of

squeeze film bearings. Much research has been conducted on the fundamentals and possible effect of stochastic models of roughness on momentum and energy. Pragana et al. [22] examined the performance of rough, porous elliptical plates in hydromagnetic squeeze film, Naduvinamani et al. [23] discussed the performance of magnetohydrodynamic squeeze film between rough, porous rectangular plates, Sundarammal et al. [24] examined the performance of MHD squeeze film between finite porous rectangular parallel plates, Ramesh et al. [25] discussed numerical solution of magnetohydrodynamic squeeze film between rough, porous rectangular plates. Their studies show that for increasing roughness and Hartmann number, pressure, load-carrying capacity, and squeeze time increase, whereas for increasing permeability parameters, these are found to decrease.

No attempt has been made to study the effect of micropolar squeeze film lubrication between elliptical plates under the application of an external magnetic field, as knowledge acquired by the researcher. The bottom plate has a pattern of porous material and roughness, and a smooth surface is on the upper plate. The two-dimensional non-Newtonian, modified hydromagnetic Reynolds equation is obtained by applying the concept of micropolar fluid and hydromagnetic flow theory along with stochastic models for rough surfaces and Darcy's law for permeability. The effect on elliptical bearings of MHD, micropolar lubricant, roughness, porosity, and aspect ratio are discussed. We also discussed the various primary effects, such as distribution of pressure, load-carrying capacity, and squeezing time. Finally, by briefly writing on the key observations and their practicality in inventing bearings, it concluded.

II. MATHEMATICAL FORMULATION OF THE PROBLEM

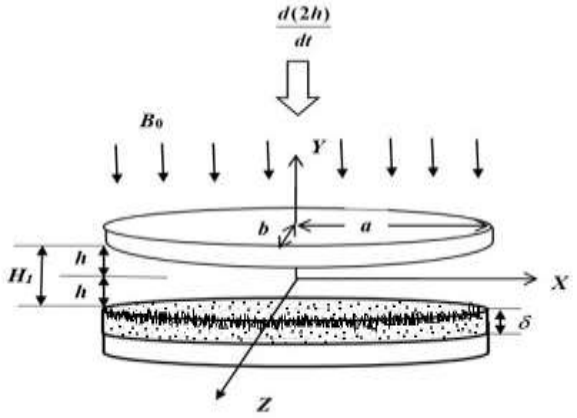

Fig.1 The physical structure of rough, porous elliptical plates with micropolar fluid under the MHD.

This structure is made up of the flow of electrically conducting viscous isothermal incompressible non-Newtonian micropolar lubricant between two elliptical plates. There is a smooth surface on the upper plate, and a fixed lower plate has a porous pattern of material and roughness. As in Figure 1, the physical squeeze film structure appears. The upper plate proceeds towards the lower plate with a constant velocity $\frac{dH_1}{dt}$. A continuous transverse magnetic field B_0 is applied in the y-direction. The thin film gap is separated by thickness H_1 is composed up of two parts as $H = H_1 + h_s(x,\xi,z)$, where $H_1 = 2h(t)$ and $h(t)$ denotes smooth part of the film geometry, h_s is a randomly varying quantity of zero mean and is a segment due to the surface asperities measured from nominal smooth level and ξ is the index parameter which determines exact roughness pattern.

Fluid inertia is assumed to be nominal, and body forces are negligible except Lorentz force. Basic regulatory equations of motion for micropolar fluid in the Cartesian-coordinate system with thin-film hydrodynamic lubrication theory are bound by these assumptions.

$$\frac{\partial u}{\partial x}+\frac{\partial v}{\partial y}+\frac{\partial w}{\partial z}=0 \qquad (1)$$

$$\left(\mu+\frac{\chi}{2}\right)\frac{\partial^2 u}{\partial y^2}+\chi\frac{\partial v_2}{\partial y}-\sigma B_0^2 u=\frac{\partial p}{\partial x} \qquad (2)$$

$$\left(\mu+\frac{\chi}{2}\right)\frac{\partial^2 w}{\partial y^2}-\chi\frac{\partial v_1}{\partial y}-\sigma B_0^2 u=\frac{\partial p}{\partial z} \quad (3)$$

$$\gamma\frac{\partial^2 v_2}{\partial y^2}-\chi\frac{\partial u}{\partial y}-2\chi v_2=0 \quad (4)$$

$$\gamma\frac{\partial^2 v_1}{\partial y^2}+\chi\frac{\partial w}{\partial y}-2\chi v_1=0 \quad (5)$$

Here variables (u,v,w) are lubricant velocity elements in the film region in the (x,y,z) directions, respectively. v_1 and v_2 Micro rotational velocity components, p represents film pressure, σ denotes electrical conductivity of the fluid, χ denote spin viscosity, γ denote viscosity co-efficient of micropolar fluid, B_0 denote magnetic field, and μ indicates Newtonian viscosity.

For the velocity elements, the necessary boundary conditions and micro rotation elements are:

At the upper rough surface side $y=h$

$$u=0,\ w=0 \text{ and } v=\frac{d(H_1)}{dt} \quad (6)$$

$$v_1=v_1=0 \quad (7)$$

At the lower porous surface side $y=-h$

$$u=0,\ w=0 \text{ and } v=v_p \quad (8)$$

$$v_1=v_2=0 \quad (9)$$

Equations (2) and (4) are solved to get the differential equation governing the velocity component u and similarly equations (3) and (5)are solved for differential equation governing the velocity component of w :

$$\frac{\partial^4 u}{\partial y^4}-\alpha\frac{\partial^2 u}{\partial y^2}+\beta u=g_1(x) \quad (10)$$

$$\frac{\partial^4 w}{\partial y^4}-\alpha\frac{\partial^2 w}{\partial y^2}+\beta w=g_2(x) \quad (11)$$

Here,

$$\alpha=\frac{4\mu\chi+2\gamma\sigma B_0^2}{\gamma(2\mu+\chi)},\ \beta=\frac{4\chi\sigma B_0^2}{\gamma(2\mu+\chi)},\ g_1(x)=\frac{-4\chi}{\gamma(2\mu+\chi)}\frac{\partial p}{\partial x},\ g_2(x)=\frac{-4\chi}{\gamma(2\mu+\chi)}\frac{\partial p}{\partial z}$$

Using boundary conditions (6) to (9), expressions were derived for u and w as

$$u=-\left\{\frac{f_2 SinhBh\left(CoshAh-CoshAy\right)-f_1 SinhAh\left(CoshBh-CoshBy\right)}{f_2 SinhBhCoshAh-f_1 SinhAhCoshBh}\right\}\frac{1}{\sigma B_0^2}\frac{\partial p}{\partial x} \quad (12)$$

$$w=-\left\{\frac{f_2 SinhBh\left(CoshAh-CoshAy\right)-f_1 SinhAh\left(CoshBh-CoshBy\right)}{f_2 SinhBhCoshAh-f_1 SinhAhCoshBh}\right\}\frac{1}{\sigma B_0^2}\frac{\partial p}{\partial z}. \quad (13)$$

Where $A=\sqrt{\frac{\alpha+\sqrt{\alpha^2-4\beta}}{2}}$, $B=\sqrt{\frac{\alpha-\sqrt{\alpha^2-4\beta}}{2}}$, $f_1=\frac{2\sigma B_0^2-(2\mu+\chi)A^2}{2\chi A}$ $f_2=\frac{2\sigma B_0^2-(2\mu+\chi)B^2}{2\chi B}$.

Integrating the equation of continuity (1) across film thickness concerning y and using boundary conditions (6) to (9), one can get a generalized hydrodynamic Reynolds equation as

$$G\left(\frac{\partial^2 p}{\partial x^2}+\frac{\partial^2 p}{\partial z^2}\right)=\frac{d(H_1)}{dt}-v_p \quad (14)$$

Here,

$$G=2\left\{\frac{Bf_2 SinhBh\left(AhCoshAh-SinhAh\right)-Af_1 SinhAh\left(BhCoshBh-SinhBh\right)}{\sigma B_0^2 AB\left(f_2 SinhBhCoshAh-f_1 SinhAhCoshBh\right)}\right\}$$

where $v_p = (u^*, v^*, w^*)$ denotes velocity component of the lubricant, which enters the porous region at the surface. The usual Darcy's law governs the velocity of the fluid through the porous area. So

$$u^* = -\frac{k}{(\mu+\chi)d^2}\frac{\partial p^*}{\partial x} \tag{15}$$

$$w^* = -\frac{k}{(\mu+\chi)d^2}\frac{\partial p^*}{\partial z} \tag{16}$$

$$v^* = -\frac{k}{(\mu+\chi)}\frac{\partial p^*}{\partial y} \tag{17}$$

Where p^* is the pressure in the porous region and $d^2 = 1 + \frac{k\sigma B_0^2}{m(\mu+\chi)}$ where k is the permeability of the porous area and *m*isthe porosity.

The continuity equation of the flow of lubricant in porous region is,

$$\frac{\partial u^*}{\partial x} + \frac{\partial v^*}{\partial y} + \frac{\partial w^*}{\partial z} = 0 \tag{18}$$

Using equations (15), (16), and (17) in equation (18) we have

$$\frac{\partial^2 p^*}{\partial x^2} + \frac{\partial^2 p^*}{\partial z^2} + d^2\frac{\partial^2 p^*}{\partial y^2} = 0 \tag{19}$$

The investigation now gives the result of Reynolds equation (14) for fluid film pressure together with Laplace equation (19) for the pressure in a porous region, with a general $\frac{\partial p^*}{\partial y}$ at the boundary. The thickness δ of the porous facing is assumed to be significantly small; the average pressure at any section of the porous region can be taken equal to the pressure in the lubricating film. Integrating the Laplace equation (19) with respect to y over the porous layer thickness δ and using the solid backing boundary condition $\frac{\partial p^*}{\partial y} = 0$ at $y = -\delta - h$, we get that

$$\left.\frac{\partial p^*}{\partial y}\right|_{y=-h} = -\frac{\delta}{d^2}\left(\frac{\partial^2 p^*}{\partial x^2} + \frac{\partial^2 p^*}{\partial z^2}\right) \tag{20}$$

Using equation $p^*(x,-h) = p(x,-h)$ and $p^*(z,-h) = p(z,-h)$ in (20), we can write,

$$v_p = \frac{k\delta}{(\mu+\chi)d^2}\left(\frac{\partial^2 p}{\partial x^2} + \frac{\partial^2 p}{\partial z^2}\right) \tag{21}$$

Substituting the value of v_p in equation (14) and simplifying

$$\frac{\partial}{\partial x}\left\{\left(G + \frac{k\delta}{(\mu+\chi)d^2}\right)\frac{\partial p}{\partial x}\right\} + \frac{\partial}{\partial z}\left\{\left(G + \frac{k\delta}{(\mu+\chi)d^2}\right)\frac{\partial p}{\partial z}\right\} = \frac{d(H_1)}{dt} \tag{22}$$

The above equation is the modified Reynolds equation that describes the MHD and porous influences in the fluid film region. To analyze the impact of roughness, we use the stochastic average of the Reynolds equation (22) as

$$\frac{\partial}{\partial x}\left\{E\left[\left(G + \frac{k\delta}{(\mu+\chi)d^2}\right)\frac{\partial p}{\partial x}\right]\right\} + \frac{\partial}{\partial z}\left\{E\left[\left(G + \frac{k\delta}{(\mu+\chi)d^2}\right)\frac{\partial p}{\partial z}\right]\right\} = \frac{d(E(H_1))}{dt} \tag{23}$$

$$\frac{\partial}{\partial x}\left\{\left(E(G) + \frac{k\delta}{(\mu+\chi)d^2}\right)\frac{\partial E(p)}{\partial x}\right\} + \frac{\partial}{\partial z}\left\{\left(E(G) + \frac{k\delta}{(\mu+\chi)d^2}\right)\frac{\partial E(p)}{\partial z}\right\} = \frac{d(E(H_1))}{dt} \tag{24}$$

Where expectancy operator $E(*)$ is given by

$$E(*) = \int_{-\infty}^{\infty} (*) f(h_s) dh_s \tag{25}$$

Where h_s represent the stochastic film thickness variable and f is its probability density function. By Christensen [21], we can accept that,

$$f(h_s)=\begin{cases}\dfrac{35}{32c^7}(c^2-h_s^2)^3, -c<h_s<c\\ 0, \qquad\qquad elsewhere\end{cases} \quad (26)$$

Here, $c=\pm 3\bar{\sigma}$ is the total range of random film thickness and $\bar{\sigma}$ is the standard deviation. There are two kinds of one-dimensional roughness pattern; they are longitudinal and transverse roughness structures. The one-dimensional longitudinal roughness is assumed to have the form of long narrow ridges and furrows running in the x direction whereas, transverse roughness is of the form of long narrow ridges and furrows running in a direction perpendicular to the direction of sliding. The present analysis is carried out only for one dimensional longitudinal roughness and one-dimensional transverse roughness can be obtained by just rotating the co-ordinate axes.

In this case the film thickness takes the form $H=H_1+h_s(x,\xi)$, then equation (24) becomes,

$$\frac{\partial}{\partial x}\left\{\left(E(G)+\frac{k\delta}{(\mu+\chi)d^2}\right)\frac{\partial E(p)}{\partial x}\right\}+\frac{\partial}{\partial z}\left\{\left(\frac{1}{E\left(\frac{1}{G}\right)}+\frac{k\delta}{(\mu+\chi)d^2}\right)\frac{\partial E(p)}{\partial z}\right\}=\frac{d(E(H_1))}{dt} \quad (27)$$

$$R_1\frac{\partial^2 E(p)}{\partial x^2}+R_2\frac{\partial^2 E(p)}{\partial z^2}=\frac{d(E(H_1))}{dt} \quad (28)$$

Where, $R=\dfrac{R_2}{R_1}$ (29)

$$R_1=E(G)+\frac{k\delta}{(\mu+\chi)d^2} \quad (30)$$

$$R_2=\frac{1}{E\left(\frac{1}{G}\right)}+\frac{k\delta}{(\mu+\chi)d^2} \quad (31)$$

$$E(G)=\frac{35}{32c^7}\int_{-c}^{c}G(c^2-h_s^2)^3dh_s \quad (31a)$$

$$E\left(\frac{1}{G}\right)=\frac{35}{32c^7}\int_{-c}^{c}\frac{(c^2-h_s^2)^3}{G}dh_s \quad (31b)$$

From (25), we have $E(H_1)=H_1$ (32)

$$\frac{\partial^2 E(p)}{\partial x^2}+R\frac{\partial^2 E(p)}{\partial z^2}=\frac{dH_1/dt}{R_1} \quad (33)$$

Boundary conditions for pressure are,

$E(p)=0$ at $x=0;a$ and $z=0;b$ (34)

Where a and b are finite dimensions of semi-major and semi-minor axes of elliptical plates in x and z directions. Outside the fluid film area, there is no difference in the pressure distribution.

Introducing the following suitable non-dimensional parameters into equation (33) and (34)

$$x^*=\frac{x}{a}, z^*=\frac{z}{b}, H^*=\frac{H}{H_0}=\frac{H_1+h_s}{H_0}=\frac{H_1}{H_0}+\frac{h_s}{H_0}=\frac{2h}{H_0}+\frac{h_s}{H_0}=H_1^*+h_s^*, a^*=\frac{a}{b},\ \psi=\frac{k\delta}{H_0^3},\ C=\frac{c}{H_0},$$

$$P^*=\frac{-E(p)H_0^3}{\mu ab\left(dH_1/dt\right)}, W^*=-\frac{E(W)H_0^3}{\mu(dH_1/dt)a^2b^2}, \delta=\frac{\delta^*}{H_0} \text{ and } T^*=\frac{E(W)H_0^2t}{\mu a^2b^2} \quad (35)$$

We get the hydrodynamic non-dimensional Reynolds equation as

$$E(G^*(H_1^*,N,L,M,\psi))\left(\frac{\partial^2 P^*}{\partial x^{*2}}+R^*\frac{\partial^2 P^*}{\partial z^{*2}}\right)=-12 \quad (36)$$

here

$$R^* = \frac{R_2^*}{R_1^*}$$

$$R_1^* = E(G^*) + \frac{12\psi}{DC^2}\left(\frac{1-N^2}{1+N^2}\right)$$

$$R_2^* = \frac{1}{E\left(\frac{1}{G^*}\right)} + \frac{12\psi}{DC^2}\left(\frac{1-N^2}{1+N^2}\right)$$

$$E\left(G^*\right) = \frac{35}{32C^7}\int_{-C}^{C} G^*(C^2 - h_s^{*^2})^3 dh_s^*$$

$$E\left(\frac{1}{G^*}\right) = \frac{35}{32C^7}\int_{-C}^{C} \frac{(C^2 - h_s^{*^2})^3}{G^*} dh_s^*$$

$$G^* = \frac{24(\xi_1 - \xi_2)}{M^2 A^* B^* \xi_3}$$

$$G^*(H_1^*, N, L, M, \psi) = G^* + \frac{12\psi}{DC^2}\left(\frac{1-N^2}{1+N^2}\right)$$

$$D = \left(1 + \frac{\psi M^2}{\delta^* m}\left(\frac{1-N^2}{1+N^2}\right)\right)$$

$$E(G^*(H_1^*, N, L, M, \psi)) = \frac{35}{32C^7}\int_{-C}^{C} E(G^*(H_1^*, N, L, M, \psi))(C^2 - h_s^*)^3 dh_s^*$$

$$\xi_1 = B^* f_2^* Sinh\left(0.5B^* H_1^*\right)\left\{0.5A^* H_1^* Cosh\left(0.5A^* H_1^*\right) - Sinh\left(0.5A^* H_1^*\right)\right\}$$

$$\xi_2 = A^* f_1^* Sinh\left(0.5A^* H_1^*\right)\left\{0.5B^* H_1^* Cosh\left(0.5B^* H_1^*\right) - Sinh\left(0.5B^* H_1^*\right)\right\}$$

$$\xi_3 = f_2^* Sinh\left(0.5B^* H_1^*\right) Cosh\left(0.5A^* H_1^*\right) - f_1^* Sinh\left(0.5A^* H_1^*\right) Cosh\left(0.5B^* H_1^*\right)$$

$$f_1^* = f_1 H_0 = \frac{M^2(1-N^2) - A^{*2}}{2N^2 A^*},\ f_2^* = f_2 H_0 = \frac{M^2(1-N^2) - B^{*2}}{2N^2 B^*}$$

$$A^* = AH_0 = \sqrt{\frac{\alpha^* + \sqrt{\alpha^{*2} - 4\beta^*}}{2}},\ B^* = BH_0 = \sqrt{\frac{\alpha^* - \sqrt{\alpha^{*2} - 4\beta^*}}{2}}$$

$$\alpha^* = \alpha H_0^2 = \frac{N^2 + M^2(1-N^2)L^2}{L^2},\ \beta^* = \beta H_0^4 = \frac{N^2 M^2}{L^2}$$

$$N = \left(\frac{\chi}{2\mu + \chi}\right)^{1/2},\ L = \frac{(\gamma/4\mu)^{1/2}}{H_0} \text{ and } M = B_0 H_0 (\sigma/\mu)^{1/2}$$

Here, *N* denotes non-Newtonian coupling number, H_0 denotes initial film thickness, *L* denotes fluid gap interacting number, *M* denotes Hartmann number,*C* represents dimensionless roughness parameter, ψ represents dimensionless permeability parameter, *a** denotes aspect ratio, x^* and z^* denotes dimensionless coordinates, H_1^* denotes non-dimensional film thickness, *P** is the dimensionless film pressure, W^* is the dimensionless load carrying capacity and T^* is the dimensionless squeeze film time.
The relevant non-dimensional boundary conditions for fluid film pressure are:

$$P^*(x_1, z_1) = 0 \text{ at } \frac{x_1^2}{a^2} + \frac{z_1^2}{b^2} = 1 \qquad (37)$$

The solution of equation (36) using boundary condition (37), one obtains the non-dimensional pressure distribution as,

$$P^* = \left(\frac{a^*}{R^* a^{*2} + 1}\right)\left(1 - x^{*2} - z^{*2}\right)\frac{6}{E\left\{G^*(H_1^*, N, L, M, \psi)\right\}} \tag{38}$$

The load-carrying capacity can be determined by integrating the film pressure equation (38)

$$W = \int_{-a}^{a} \int_{-\frac{b}{a}\sqrt{a^2 - x_1^2}}^{\frac{b}{a}\sqrt{a^2 - x_1^2}} p dz_1 dx_1$$

The dimensionless carrying capacity can be obtained as

$$W^* = -\frac{WH_0^3}{\mu(d(2h)/dt)a^2b^2} = \left(\frac{a^*}{R^* a^{*2} + 1}\right)\frac{3}{E\left\{G^*(H_1^*, N, L, M, \psi)\right\}} \tag{39}$$

Time height relation, that is, the time taken by the upper plate to reach film thickness H_1, is calculated in non-dimensional form using the condition $H_1^* = 1$ at $T^* = 0$

$$T^* = \left(\frac{a^*}{R^* a^{*2} + 1}\right)\int_{H_1^*}^{1} \frac{3}{E\left\{G^*(H_1^*, N, L, M, \psi)\right\}} dH_1^* \tag{40}$$

III. Results and Discussion

In the presence of an external transverse magnetic field, a streamlined mathematical model was developed to experiment with the effects of surface roughness and micropolar lubricant between two elliptical plates in which a smooth surface is on the upper plate and a porous material and roughness pattern is on the fixed lower plate. Bearing lubrication characteristics such as squeeze film pressure *P**, load-carrying capacity *W**, and squeezing time *T** are acquired as functions of Hartmann number *M* (magnetization parameter), roughness parameter *C,* porosity ψ , aspect ratio *a*,* non-Newtonian coupling number *N*, film thickness H_1^* and fluid gap interacting number *L*, as shown in graphs 2-13. Excellent agreement on the basic values of non-dimensional parameters was developed in the following limiting cases.

Table.1: Comparison of Brinda Halambi and Hanumagowda [5] with the present analysis for different values of *L* when *N* = 0.4, H_1^* = 0.5 and *a = 1.2.**

	M	Brinda Halambi and Hanumagowda [5]		Present analysis ($\psi \to 0, C \to 0$)	
		L = 0	*L* = 0.1	*L* = 0	*L* = 0.1
*P**	0	23.6136	27.7867	23.6136	27.7867
	4	33.019	37.2015	33.019	37.2015
*W**	0	11.8068	13.8934	11.8068	13.8934
	4	16.5037	18.6007	16.5037	18.6007
*T**	0	73.0705	86.7843	73.0705	86.7842
	4	78.4824	92.2053	78.4824	92.2053

Table.2: Comparison between Roopa et.al [12], Roopa et.al [18] and the current research with *L*= 0.05, H_1^* = 0.5, and *a= 1.2 for different *N* values**

	N	Roopa *et.al* [20]		Present analysis ($M \to 0, C \to 0$)	
		ψ = 0	ψ = 0.1	ψ = 0	ψ = 0.1
*P**	0	23.6066	2.2270	23.6066	2.2270
	0.5	28.9321	3.58984	28.9321	3.5898
*W**	0	11.8033	1.1152	11.8033	1.1152
	0.5	14.4661	1.7964	14.4661	1.7964

T^*	0	73.0553	0.9286	73.0553	0.9286
	0.5	95.6147	1.4689	95.6147	1.4689

(i) When the surface is smooth ($C \to 0$) and impermeable ($\psi \to 0$), an excellent rapport between the present study findings and that of Brinda Halambi and Hanumagowda [5] has been obtained.
(ii) An excellent finding has been found between the present study and that of Roopa et al.[20] when fluid flow is nonmagnetic ($M \to 0$) and the surface is smooth ($C \to 0$)
The comparative study of (i) is shown in table.1 for different M values and (ii) is shown in table.2 for different N values. For the following non-dimensional values, analysis of the experiment is taken.
ψ = 0 to 0.1 M = 0 to 8 N = 0 to 0.8 L = 0 to 0.3 H_1^*= 0.5 to 0.9 a^* = 0.1 to 10.

Squeeze film pressure: Figure.2 is a variation of pressure P^* as a function of coordinate x^* for distinct values of C and ψ carrying all the other variables unchanged. The figure shows that the roughness parameter C increases the distribution of pressure in contrast to a smooth surface ($C = 0$). This is because of surface asperities that minimize the fluid's sideways leakage and decrease the fluid's velocity. So, in the fluid film area, huge quantities of fluid are stored and that creates a huge distribution of pressure. Also, it is noted that effect of porosity ψ is to decrease the squeeze film pressure P^*. The leading path for fluid flow was set off by pores on the porous face. This reduces the amount of fluid in the film region; hence pressure built-up is also decreased. Figure.3 is a deviation of pressure P^* as a function of coordinate x^* for distinct values of C and Mcarrying all the other variables constant for micropolar lubricant. It is observed from the figure that magnetic field M can support more pressure distribution in fluid film region as compared non-magnetic case ($M = 0$) respectively. As in case of roughness the applied magnetic field normal to the flow also minimizes the velocity of lubricant. So, flowing out of the lubricant of the elliptical plates was reduced and more fluid is retained in fluid film region, due to which pressure rise also increased. As M increases squeeze film pressure increases again. Figure.4 and figure.5 is a depiction of pressure P^* as a function of coordinate x^* for distinct values of C and $N$and C and Lrespectively, carrying all the other variables constant for micropolar lubricant. From both the graphs it is seen that squeeze film pressure P^* increases for non-Newtonian fluid as compared to Newtonian case (N=0 and L=0) respectively; and higher enlargement are observed with enhanced values of non-Newtonian coupling number N and fluid gap interacting number L again. This is because non-Newtonian micropolar lubricant provides additional opposition to the moving fluid. The substantial quantity of fluid would remain in the region, which generates large pressure distribution.
Load carrying capacity: Figure.6 presents the variation of W^* with respect to $log_{10}(a^*)$ for different values of C and M carrying all the other variables constant for micro polar lubricant. It is noticed from the graph thatroughness C and magnetic field M can strengthen more load carrying capacity in fluid film region as compared to smooth surface ($C = 0$) and non-magnetic case ($M = 0$) respectively. As described in the foregoing segment,

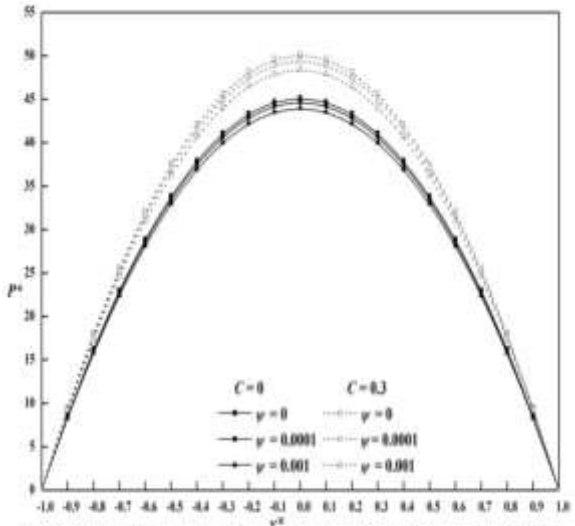

Fig.2 Non dimensional pressure P^* variation with non dimensional coordinate x^* for different values of C and ψ with $N = 0.3$, $L = 0.2$, $H_1^* = 0.5$, $a^* = 1.4$, $m = 0.06$, $\delta = 0.1$, $M = 6$ and $z^* = 0$.

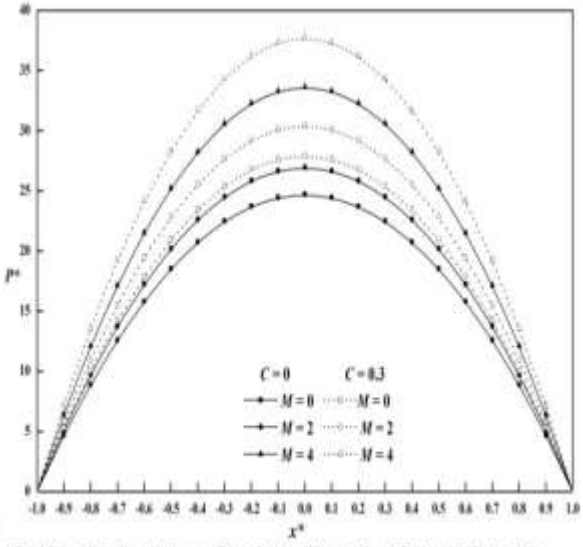

Fig.3 Non dimensional pressure P^* variation with non dimensional coordinate x^* for different values of C and M with $L = 0.2$, $\psi = 0.0001$, $H_1^* = 0.5$, $a^* = 1.4$, $N = 0.3$, $m = 0.06$, $\delta = 0.1$ and $z^* = 0$.

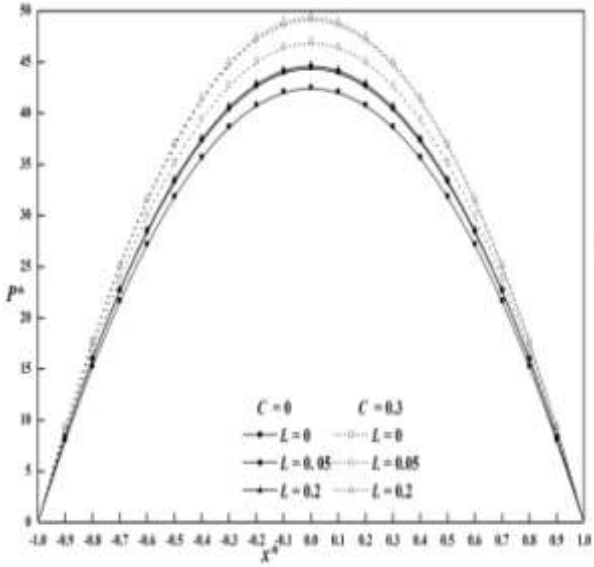

Fig.5 Non dimensional pressure P^* variation with non dimensional coordinate x^* for different values of C and L with $N = 0.3$, $M = 6$, $H_1^* = 0.5$, $a^* = 1.4$, $\psi = 0.0001$, $m = 0.06$, $\delta = 0.1$ and $z^* = 0$.

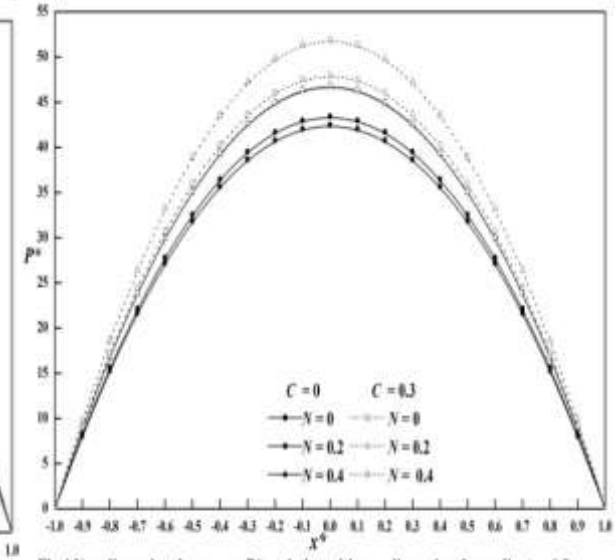

Fig.4 Non dimensional pressure P^* variation with non dimensional coordinate x^* for different values of C and N with $M = 6$, $H_1^* = 0.5$, $L = 0.2$, $a^* = 1.4$, $\psi = 0.0001$, $m = 0.06$, $\delta = 0.1$ and $z^* = 0$.

impacts of roughness and magnetization parameter are to decrease the velocity of the fluid; as an outcome pressure distribution rises in the fluid film region which produces an enhancement in load capacity of the bearings. An increment in the values of M produces fluid to gain more magnetization which in turn interacts with the magnetic field imposed. This fluid builds more pressure distribution therefore load carrying capacity also improved for larger values of M. It is exciting to record that there occurs a critical value a_c^* of the aspect ratio a^* at which the influence of roughness vanishes. At a critical value a_c^* impact of roughness is to improve load carrying capacity for $a^* > a_c^*$ and the movement is interchanged for $a^* < a_c^*$. Also, the same tendency has been noticed for other two magnetic fields. Figure.7 and figure.9 describes the variation of W^* with respect to $log_{10}(a^*)$ for different values of C and N and C and L respectively, carrying all the other variables constant for micro polar lubricant. Both the graphs show that as roughness increases the load carrying capacity Increases. The influence of micro polar non-Newtonian fluid is to enhance the load carrying capacity compared to Newtonian case ($N = 0$ or $L = 0$). It is noticed that load capacity is increased with increasing values of non- Newtonian coupling number N and non – Newtonian fluid gap interacting number L. Figure.8 is a plot of the variation of W^*

with respect to $log_{10}(a^*)$ for different values of ψ and C carrying all the other variables constant for micro polar lubricant. It is observed that load carrying capacity decreases with respect to porosity as compared to impermeable case (ψ = 0). It is credited to the effect of decreased squeeze film pressure for porous fluid film region. Also, it is noticed that load carrying capacity is increased for roughness parameter C as compared to smooth case (C = 0) and larger values of C also increases load carrying capacity.

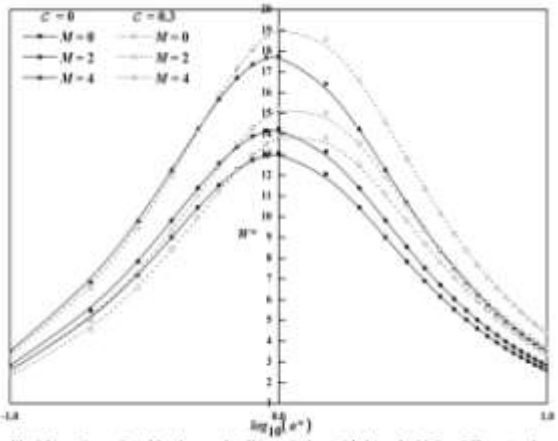

Fig.6 Non dimensional load capacity W^* variation with $log_{10}(a^*)$ for different values of C and M with L = 0.2, N = 0.3, ψ = 0.0001, m = 0.06, δ = 0.1 and H_1^* = 0.5.

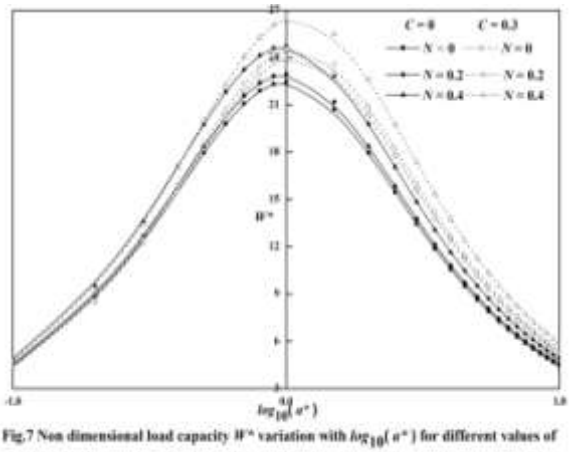

Fig.7 Non dimensional load capacity W^* variation with $log_{10}(a^*)$ for different values of C and N with L = 0.2, H_1^* = 0.5, ψ = 0.0001, m = 0.06, δ = 0.1 and M = 6.

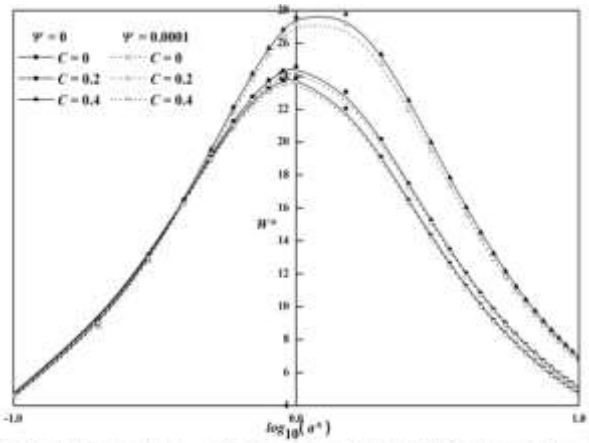

Fig.8 Non dimensional load capacity W^* variation with $log_{10}(a^*)$ for different values of ψ and C with L = 0.2, M = 6, N = 0.3, m = 0.06, δ = 0.1 and H_1^* = 0.5.

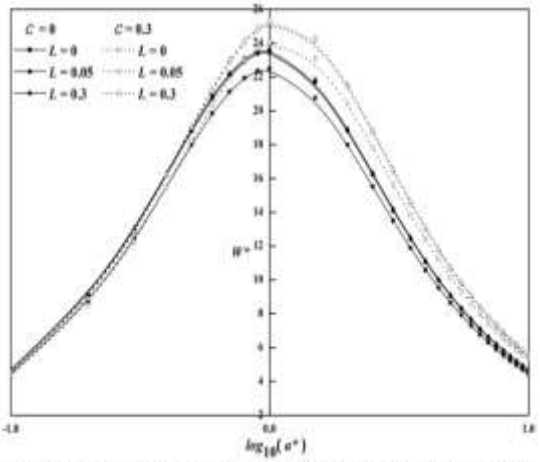

Fig.9 Non dimensional load capacity W^* variation with $log_{10}(a^*)$ for different values of C and L with ψ = 0.0001, M = 6, N = 0.3, m =0.06, δ = 0.1 and H_1^* = 0.5.

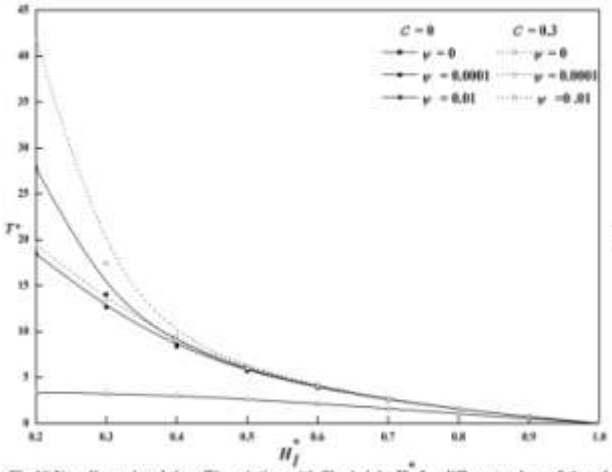

Fig.10 Non dimensional time T^* variation with film height H_1^* for different values of C and ψ with L = 0.2, N = 0.3, M = 6, m = 0.06, δ = 0.1 and a^* = 1.4.

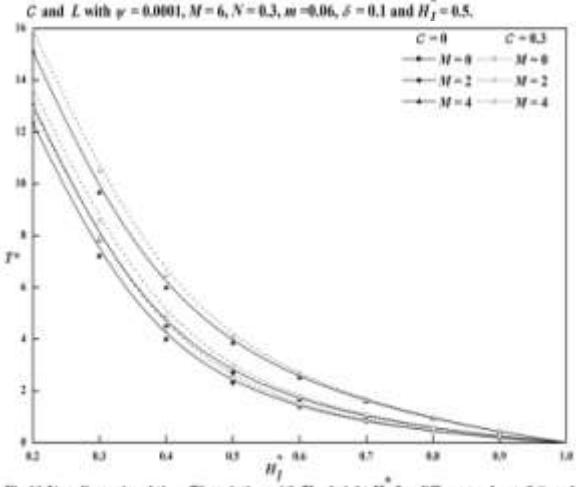

Fig.11 Non dimensional time T^* variation with film height H_1^* for different values of C and M with L = 0.2, N = 0.3, ψ = 0.0001, m = 0.06, δ = 0.1 and a^* = 1.4.

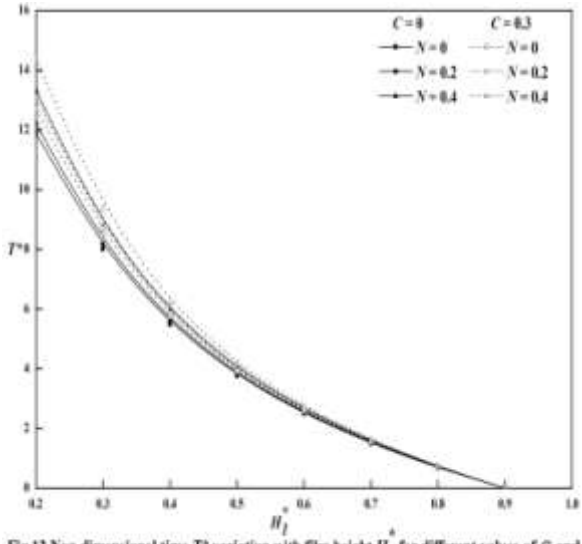

Fig.12 Non dimensional time T^* variation with film height H_1^* for different values of C and N with $L = 0.2$, $M = 6$, $\psi = 0.0001$, $m = 0.06$, $\delta = 0.1$ and $a^* = 1.4$.

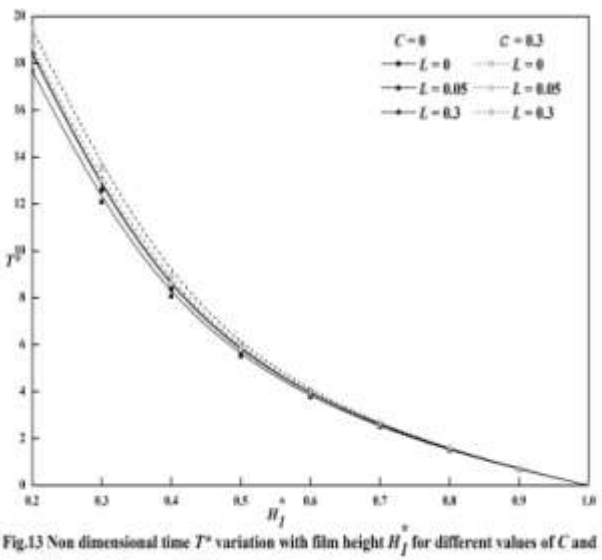

Fig.13 Non dimensional time T^* variation with film height H_1^* for different values of C and L with $N = 0.3$, $M = 6$, $\psi = 0.0001$, $m = 0.06$, $\delta = 0.1$ and $a^* = 1.4$.

Squeezing film time: Figure.10, figure.11, figure.12 and figure.13 are the variation of T^* as a function of H_1^* for distinct values of C and ψ, C and M, C and N, and C and L respectively, carrying all the other variables constant. These graphs show that squeezing time reduces as film height increases. Also noted that impact of roughness parameter C is to lengthen the squeeze time of approach compared to smooth case ($C = 0$). It is observed from figure.10 that the influence of permeability parameter is to reduce the squeezing time for both rough and smooth surface and for increasing ψ, the squeezing time decreases. Figure.11 shows that applied magnetic field M increases squeeze film time as compared to non- magnetic case ($M = 0$). Also, as Hartmann number increases the squeeze time also increases. The applied magnetic field prevents fluid flow in the film region. So, flowing out of the lubricant of the elliptical plates was reduced and more fluid is retained in fluid film region. Thus, the magnetic field provides the lengthened squeeze time of approach of the upper plate which reduces the coefficient of friction. The nearer effects also have been noticed from figure.12 and figure.13, in which the impact of non - Newtonian parameter N and L are to improve squeeze time compared to Newtonian case ($N = 0$ or $L=0$). It is noticed that squeeze time is increased with increasing values of non - Newtonian coupling number N and non - Newtonian fluid gap interacting number L.

IV. CONCLUSIONS

The effect of surface roughness and micropolar lubricant between two elliptical plates in which the upper plate has a smooth surface and a fixed lower bearing has a roughness pattern and porous material is determined by applying the principle of micropolar fluid and hydromagnetic flow theory together with stochastic models for rough surfaces and Darcy law. Subsequent assumptions are drawn as a result.

- An important effect is the magnetic field and surface roughness. Compared to smooth and non magnetic cases, they noticeably impart much needed higher squeeze film pressure, load- carrying capacity, and squeeze time. For larger parameters of roughness (C) and Hartmann number (M) lubrication characteristics are also recorded to increase.
- As compared to the impermeable case, the effect of the permeability parameter is to reduce the lubrication characteristics. In addition, these features decrease with increasing permeability parameters (ψ).
- For larger values of non-Newtonian coupling number (N) and fluid gap interacting number (L) bearing characteristics are found to increase.
- Compared to the corresponding Newtonian lubricant, lubrication properties for micropolar lubricant have improved significantly..
- The current study results compare favorably with those of Brinda Halambi and Hanumagowda [5] ($\psi \to 0, C \to 0$) and Roopa et al. [20] ($C \to 0, M \to 0$)

In general, these guidelines allow designers to choose the correct magnetic field and aspect ratio for a given roughness and permeability through which the bearings can be guaranteed to operate effectively.

REFERENCES

[1] Kuzma, D.C. (1964).*Magnetohydrodynamic squeeze films*. Journal of Basic Engineering, ASME. 86(3): 441- 444. doi:10.1115/1.3653131

[2] Kuzma, D.C. Maki E.R.&Donnelly, R.J. (1964). *The Magnetohydrodynamic squeeze films*. Journal of Fluid Mechanics. 19(3): 395-400. doi: 10.1017/S0022112064000805

[3] Shukla, J.B. (1965). Hydromagnetic theory of squeeze films. Journal of Basic Engineering, ASME. 87: 142-144. doi:10.1.1.1058.4294

[4] Bujurke, N.M.&Kudenatti, R.B. (2007). *MHD Lubrication flow between rough rectangular plates Fluid mechanics research.* 39(4): 334-345.doi: 10.1016/j.fluiddyn.2006.05.004

[5] Brinda Halambi, &Hanumagowda, B. N. (2018).*Effect of hydromagnetic squeeze film lubrication of micropolar fluid between two elliptical plates*. International Journal of Mechanical Engineering and Technology. 9(8): 939-947.

[6] Lin, J.R. (2003). *Magnetohydrodynamics squeeze film characteristics for finite rectangular plates*. Industrial Lubrication and Tribology. 55(2): 84-89. doi:10.1108/00368790310470912

[7] Naduvinamani, N.B., Fathima, S.T. & Hanumagowda, B.N. (2010).*Magnetohydrodynamic couple stress squeeze film lubrication of circular stepped plates*. Journal of Engineering Tribology. 225: 111-119. doi:10.1177/1350650110397460

[8] Naduvinamani, N.B. &Rajashekar, M. (2011). MHD couple stress squeeze film characteristics between sphere and plan surface. Tribology-Materials, Surfaces &Interfaces.5(3): 94-99. doi:10.1179/1751584X11Y.0000000011

[9] Lin, J.R. (2002).*Magnetohydrodynamics lubrication for finite slider bearings*. International Journal of Applied Mechanics and Engineering. 7(4): 1229-1246. doi: BPZ2-0001-0065

[10] Hamza, A. (1988). *The magnetohydrodynamics squeeze films*. Journal of Tribology Technical Briefs 1988; 110(110): 375-380.

[11] Eringen, A.C. (1966). Theory of micropolar fluids. Journal of Mathematics and Mechanics. 16(1): 1-18. doi: 24901466

[12] Vinoth Kumar V, Ramamoorthy S, Dhilip Kumar V, Prabu M, Balajee J.M., *"Design and Evaluation of Wi-Fi Offloading Mechanism in Heterogeneous Network*", International Journal of e-Collaboration (IJeC), IGI Global, 17(1), 2020.

[13] Shukla, J.B.,& Isa, M. (1974).*Characteristics of non-Newtonian power-law lubricants in step bearings and hydrostatic step seals*. Wear. 30(1): 51-71. doi: 004316487490057X

[14] Roopa RajashekarAnagod, Hanumagowda, B.N., &Santhosh Kumar J. (2018).*Effect of micropolar fluids on the squeeze film elliptical plates*. Journal of Physics - IOP conference series.2018; 1000: 1-18.doi: 10.1088/1742-6596/1000/1/012098

[15] Naduvinamani, N.B.,&Huggi, S.S. (2009).*Micropolar squeeze film lubrication of short partial porous journal bearings*. Proceedings of Institution of Mechanical Engineers. Journal of Engineering Tribology. 2009; 223(8): 1179-1185. doi: 10.1243/13506501JET627

[16] Basheer, S., Anbarasi, M., Sakshi, D.G. & Vinoth Kumar V., Efficient text summarization method for blind people using text mining techniques. Int J Speech Technol (2020). https://doi.org/10.1007/s10772-020-09712-z

[17] Siddangouda, A. & Patil, S.B. (2018). *Non-Newtonian effects on squeeze film lubrication between porous stepped circular plates*. International Journal of Mathematical Archive. 9: 33-42.

[18] Prawal Singh& Chandan Singh. (1982).*Micropolar squeeze films in porous hemispherical bearings.* International Journal of Mechanical Sciences. 24(8): 509-518. doi: 0020740382900601

[19] Isa, M. &Zaheeruddin, K.H. (1980).*One-dimensional porous journal bearings lubrication with micropolar fluid*, Wear. 63(2): 257-270 doi: 004316488090054X

[20] Roopa RajashekarAnagod, Santhosh Kumar, J. & Hanumagowda, B.N. *Analysis of porous elliptical plates with micropolar fluids*. International Journal of Mechanical Engineering and Technology 2018;12: 962-973.

[21] Christensen, H. (1969-1970). *Stochastic Models for Hydrodynamic Lubrication of Rough Surfaces*. Proceedings of the Institution of Mechanical Engineers. 1969-1970; 184 (1):1013-22. doi:10.1243/PIME_PROC_1969_184_074_02.

[22] Pragna, A.Vadher, GunamaniDehari, Rakesh, M. Patel. (2008).*The effect of surface roughness in hydromagnetic squeeze films' performance between two conducting rough, porous elliptical plates*. Turkish Journal of Engineering & Environmental Sciences. 32: 219-227.

[23] Naduvinamani, N.B., Syeda Tasneem Fatima& Salma Jamal. (2010). *Effect of roughness on hydromagnetic squeeze films between porous rectangular plates*. Tribology International. 43(11): 2145-2151. doi: 10.1016/j.triboint.2010.06.002

[24] Umamaheswaran, S., Lakshmanan, R., Vinothkumar, V. et al. *New and robust composite micro structure descriptor (CMSD) for CBIR*. International Journal of Speech Technology (2019), Vol. 23, Issue 2, pp. 243-249[25] Ramesh, B.Kudanatti, Shalini, M. Patil&Dinesh, P.A.(2013). Vinay CV. Numerical study of surface roughness and magnetic flied between rough and porous rectangular plates. Mathematical Problems in Engineering. Article ID 915781: 8 pages. doi:/10.1155/2013/915781

[26] Naduvinamani, N.B.,Hanumagowda, B.N. & Fatima, S.T. (2012). *Combined effects of MHD and surface roughness on couple stress squeeze film lubrication between porous circular stepped plates*. Tribology International. 2012; 56: 19-29. doi:/10.1016/j.triboint.2012.06.012

[27] Fatima, S.T., Naduvinamani, N.B. & Santhosh Kumar, J. & Hanumagowda, B.N. (2014).*Derivation of modified MHD-Stochastic Reynolds equation with conducting couple stress fluid on the squeeze film lubrication of porous, rough elliptical plates*. International Journal of Mathematical Archive 2014; 5: 135-145.